

## Article

# Dynamic Quadrilateral Characteristic-Based Distance Relays for Transmission Lines Equipped with TCSC

Ghada M. Abo-Hamad <sup>1</sup>, Doaa Khalil Ibrahim <sup>1</sup>, Essam Aboul Zahab <sup>1</sup> and Ahmed F. Zobaa <sup>2,\*</sup>

<sup>1</sup> Department of Electrical Power Engineering, Faculty of Engineering, Cairo University, Giza 12613, Egypt; dody\_benhamed@yahoo.com (G.M.A.-H.); doaakhalil73@eng.cu.edu.eg (D.K.I.); zahab0@eng.cu.edu.eg (E.A.Z.)

<sup>2</sup> College of Engineering, Design and Physical Sciences, Brunel University London, Uxbridge UB8 3PH, UK

\* Correspondence: azobaa@ieee.org

**Abstract:** A two-fold adaptive dynamic quadrilateral relay is developed in this research for protecting Thyristor-Controlled Series Compensator (TCSC)-compensated transmission lines (TLs). By investigating a new tilt angle and modifying the Takagi method to recognize the fault zone identifier, the proposed relay adapts its reactive reach and resistive reach separately and independently. The investigated tilt angle and identified fault zone use the TCSC reactance to compensate its effect on the TL parameters and system homogeneity. Excessive tests are simulated by MATLAB on the non-homogenous network, IEEE-9 bus system and further tests are carried out on IEEE-39 bus system in order to generalize and validate the efficiency of the proposed approach. The designed trip boundaries are able to detect wide range of resistive faults under all TCSC modes of operations. The proposed approach is easy to implement as there no need for data synchronization or a high level of computation and filtration. Moreover, the proposed adaptive dynamic relay can be applied for non-homogeneity systems and short as well as long TLs which are either TCSC-compensated or -uncompensated TLs.

**Keywords:** distance relay; fault resistance; quadrilateral characteristic; resistance and reactance elements; Thyristor Controlled Series Compensator (TCSC)



**Citation:** Abo-Hamad, G.M.; Ibrahim, D.K.; Aboul Zahab, E.; Zobaa, A.F. Dynamic Quadrilateral Characteristic-Based Distance Relays for Transmission Lines Equipped with TCSC. *Energies* **2021**, *14*, 7074. <https://doi.org/10.3390/en14217074>

Academic Editor: Andrea Mariscotti

Received: 29 September 2021

Accepted: 25 October 2021

Published: 28 October 2021

**Publisher's Note:** MDPI stays neutral with regard to jurisdictional claims in published maps and institutional affiliations.



**Copyright:** © 2021 by the authors. Licensee MDPI, Basel, Switzerland. This article is an open access article distributed under the terms and conditions of the Creative Commons Attribution (CC BY) license (<https://creativecommons.org/licenses/by/4.0/>).

## 1. Introduction

The value of fault resistance inserted by short circuits has a significant impact on the performance of distance relaying devices protecting transmission lines (TLs). Therefore, it becomes a challenge to choose the appropriate characteristic to cover all protection requirement issues. The reactance relays are not affected by the line resistance, but, unfortunately, the reactance relay is non-directional relay, and it is impossible to add a directional element to it, as in such case the relay will operate under normal operating conditions if the system operates at or around a unity power factor. For this purpose, the reactance relay with directional features is modified into the Mho or admittance characteristic [1]. Although the Mho relay is preferable in the protection of TLs, as it has inherently directional features, its characteristics are still restricted under high fault resistance conditions. On the other hand, the key advantages of the quadrilateral relay are the trip coverage area for grounded resistive faults and the “reach” of the resistance and reactance elements which can be independently controlled; however, it is affected by the system non-homogeneity [2].

FACTS (Flexible Alternating Current Transmission System) devices are one of the magic solutions installed in the electrical grid to enhance controllability of the network. FACTS controllers can be categorized into series-connected controllers, shunt-connected controllers, series-series connected controllers, and series-shunt connected controllers [3]. Series compensation (SC) is the most common technique used in TLs, as it not only improves system transient stability, controls voltage and power flow, but also increases power transferring capacity, and decreases losses [4]. A Thyristor-Controlled Series Compensator

(TCSC) provides better control over fixed SC for a TL power flow. However, unfortunately the integration of TCSC in TL affects its protection ability significantly due to the abrupt line parameters changes. This will lead to defects in the apparent impedance measured by the distance relays that cause overreaching/underreaching of the relays.

The research studies of [5,6] have considered the effect of FACTS as well as TCSC on the quadrilateral relay. In [5], the impedance measured by the relay is evaluated considering TCSC at the near end of the TL. Nonetheless, the homogeneity of the system, fault types, fault location, and TCSC modelling are not considered in this evaluation. The impact of series-distributed FACTS on the tilt angle setting of the quadrilateral characteristic and how it may affect the coverage of fault resistance by overreaching/underreaching are discussed in [5].

Other published efforts in [7–9] have presented the factors that should be considered in designing the setting of the quadrilateral relay to eliminate the errors due to fault conditions. In [7], the influence of the fault resistance and tilt angle on the quadrilateral characteristic equations is presented. The considerations of the phase and ground elements for the phase comparator quadrilateral relay are proposed in [8]. The influence of phase angle errors on the polarizing signal of zone-1 quadrilateral distance elements is introduced in [9]. The study demonstrated the reactive reach setting limit for a given maximum expected polarization phase angle which, beyond the resistive reach, may lose security for resistive faults.

In [10–12], the resistive reach is adapted based on the measured impedance by the relay and circuit theory approach. By using the impedance measurements from two-line ends, the fault resistance is calculated from a second order equation in [10]. The validation results for this scheme are obtained for zone-1 only so, the results for back-up protection zones and under communication failure are unclear. A standalone adaptive distance protection is also proposed in [10], where the fault resistance is calculated by the slope tracker method considering constant X/R ratio not only for the primary protected line but also for the adjacent line, which may be an inappropriate method for interconnected TLs. Furthermore, the results show the limitation of fault resistance coverage up to 50  $\Omega$  in zone-1 and up to 20  $\Omega$  for back-up zones of protection. The four boundary lines of a numerical quadrilateral characteristic are obtained in [12] by computer simulation under different changes in system configuration. However, that study does not describe the methodology followed to adapt the reaches of the characteristics; moreover, the simplicity of the radial system used in the simulation may reduce the accuracy of results, especially as the results are limited to the primary zone of protection. Despite of the simplicity of this technique, the unfaithful model of the FACTS device or the approximate data infeed to the relay, affected by the TL parameters, may introduce error into the apparent impedance calculations.

The third zone setting of a quadrilateral relay is adapted in [13] by using the variation mode decomposition approach to decompose the local end current signal into different modes. The apparent impedance and energy index that are calculated from the signal extracted from the third mode are used to detect the third zone's symmetrical and asymmetrical faults. Generally, the multi-filtering techniques are performed with high sampling rates and the extra calculation burden on the relay is significant.

Furthermore, the construction of tripping boundaries of the adaptive quadrilateral relay by the optimization technique is developed in [14–17]. By considering the probabilistic behaviour of the random variables that affect the apparent impedance seen by the relays, optimal settings of quadrilateral relay zones are developed in [14]. Unfortunately, this approach will be affected by the selected weight used for the constraints that may increase the reach of protection zones or loss of selectivity. Constructing the boundary of the first distance protection zone for SC-TL with an optimization-based algorithm is introduced in [15]. The reach of the protection zone can be maximized by solving a number of scaled optimization problems in order to construct a tripping boundary. For that algorithm, the selective weights of the fault resistance bounds are obtained from the historical data and the

reactance of SC is assumed to be available all time. Additionally, the scaled optimization problems rely on some assumptions such as recognizing the grid parameters that affect the algorithm robustness significantly. In [16], a multi-objective optimization problem, solved by the sine–cosine algorithm to obtain the reach setting of the quadrilateral relay, is proposed. The lack of the details used to set the parameters of the methodology according to the application limits of distance protection relays to TLs is a key disadvantage of this approach.

A genetic algorithm for determining the reach settings of the quadrilateral distance protection element of mutually coupled TLs is also illustrated in [17]. The algorithm uses different faulty system conditions affecting the measured impedance as the variable input. However, there is no information about fault resistance estimation and the method is only simulated for the primary protected zone. There is no doubt that the higher computational times for the number of iterations and the accuracy of the results that rely on the data required from the system make the choice of optimization techniques challenging.

Generally, the application of different nature-inspired metaheuristics is prevalent in different design optimization missions. However, all of the optimization algorithms are dependent on parameters that are significantly affected by the question of the best values or settings and how to tune these parameters to achieve the best performance; in particular, there is no unified mathematical definition of robustness. Moreover, the selection of the appropriate nature-inspired metaheuristic and the benchmarking are also an open challenging problem, due to the “no free lunch” theorem of mathematical optimization [18].

The communication-based scheme is another philosophy used in protective relaying to meet the TLs’ requirements, as proposed in [19–21]. An adaptive relay setting algorithm for a series-compensated line with a capacitor protected by Metal Oxide Varistors (MOV) is proposed in [19]. It computes the seen impedance by considering the local and remote end relays’ active power, voltage and current. The series compensation model and the restriction of the fault resistance coverage area to only 10  $\Omega$  may weaken the scheme performance. Another solution for setting the adaptive quadrilateral relay, protecting TL-possessing series capacitor protected by MOV, is demonstrated in [20]. The seen impedance is computed from the local information available at the relay. The unknown fault resistance value can be compensated by using the superposition principle on the obtained active power from both ends of TL at the fault instant. However, the study has approximated the SC with the MOV model of linear impedance, which may affect the accuracy of the results. A modified transfer trip scheme is developed in [21] to eliminate the overreach problem facing the distance relay under SC without any guarantee of the scheme’s effectiveness in the case of fault resistance and communication failure. There is no doubt that the cost, speed and reliability of the communication systems are vital factors that must be considered before implementing communication-based schemes. Moreover, synchronized data-based schemes overburden the relays, and communication failure may lead to complete failure of relays.

Another category of adaptive relays uses the concept of reducing the zone-1 setting and delaying zone-2 as per the fault conditions [22–25]. Switching off zone-1 and increasing the zone-2 time to alleviate SC effect of TLs is presented in [22]. An adaptive relay for SC-TL is also suggested in [23], where the reach of an instantaneous zone-1 is reduced to 67% of TL length and another delayed zone-1 is reconstructed after two cycles from the fault inception approach. For TCSC-compensated TL, the idea of reducing the zone-1 reach setting and delaying zone-2, to improve the conventional relay, is introduced in [24,25]. The validation results in the last two schemes ignore the fault resistance effect. Above all, the intrinsic demerits of this concept are the delayed fault clearance time, the high-speed TL parameters’ estimation requirement, alongside the need for efficient modelling of the compensated device.

Generally, the chronological trend of research studies obviously shows the increasing concern of research for more and more improved protection schemes for TCSC-compensated TLs. For this reason, in this paper, an adaptive dynamic quadrilateral relay

compatible with the compensated TCSC interconnected with TLs is proposed. The main objective of this scheme is to adapt the reactive and resistive reach of the setting based on the circuit theory and the impedance measured by the relay. The quadrilateral characteristic dynamically moves upward/downward reliant on the TCSC mode of operation and the tilt angle, moving the right side depending on the existence of fault resistance. The proposed approach is extensively evaluated by using the Matlab simulator program for TCSC-compensated interconnected TL systems under high fault resistance in both the inductive and capacitive TCSC modes of operation. For the purpose of generalizing the methodology, the tests are applied on non-homogeneous TL systems, which are long TLs of the IEEE-9 bus system and repeated on short TLs of the IEEE-39 bus network. Additionally, the results are compared with respect to the latest research studies.

Therefore, the contribution of this paper can be summarized as follows:

- An adaptive dynamic quadrilateral distance relay is proposed to accurately detect the high resistive faults under TCSC-compensated TLs.
- A new tilt angle estimation is investigated which uses TCSC reactance to compensate for the non-homogeneity effect due to the presence of TCSC in the faulted loop.
- The proposed method applies the modified Takagi method to propose the fault zone identified, which is used to adapt the resistive reach.
- The adaptation of the relay setting reaches for TCSC-compensated TLs is based on the local data estimated at the relay terminal and two values of RMS current and firing angle transmitted from the TCSC substation, upon a fault-starting recognition signal occurring.
- Finally, the proposed approach is easily implemented as it can be applied by modifying the conventional relay algorithm without any high level of filtrations or excessive computational tools.

The remainder of the paper is arranged as follows: in Section 2, the TCSC effect on the distance relay, and the practical modelling of its impedance are briefly presented. The proposed methodology is fully described in Section 3. The scheme validation and achieved results on both IEEE-tested systems are illustrated in detail in Section 4. The discussion of the advantages of the proposed adaptive relay compared with other relays and conclusions are summarized in Sections 5 and 6, respectively.

## 2. Thyristor-Controlled Series Compensator (TCSC)

As is known, TCSC provides better control over TL power flow than fixed SC, so the paper will focus on identifying and mitigating the effect of TCSC on TL distance protection.

The TCSC characteristic and its operational mode are very well explained in [26,27]. For faulty conditions, TCSC controller system reacts rapidly to take preventive measures and TCSC operates under different modes depending on the fault type. For different fault scenarios, Table 1 summarizes the protection performance under different TCSC operation modes [28].

**Table 1.** Distance relays performance for TCSC-compensated TLs under faulty conditions.

TCSC Mode	Fault Conditions	Distance Relay Behaviour
Bypass mode	Excessive high fault current	Underreach
Circuit breaker bypass	The fault is not cleared in the instantaneous tripping zone	Slight underreach in some cases
Capacitive mode without MOV	High impedance fault	Overreach
Capacitive mode with MOV	High fault current	Slight overreach
Blocking mode	Transient fault	Overreach

When a fault occurs close to TCSC, the high fault current is enough to conduct the MOV. Therefore, the equivalent capacitive reactance of TCSC decreases due to MOV. As a result, the possibility of experiencing voltage and current inversion is quite low during the fault. In addition, TCSC could be changed from the capacitive mode into the bypass mode

if the very high fault current flows through TCSC to prevent damage of the MOV and series capacitor. In this mode, the TCSC impedance is a pure inductance. Therefore, the inversion phenomenon never occurs, and the distance relay experiences slight under-reaching [25].

Figure 1 introduces the errors due to presence of TCSC in the fault loop for different modes of operations by simulating an L-G fault at the 2 s timepoint and changing the firing angle ( $\alpha$ ) in order to apply different TCSC operating modes.

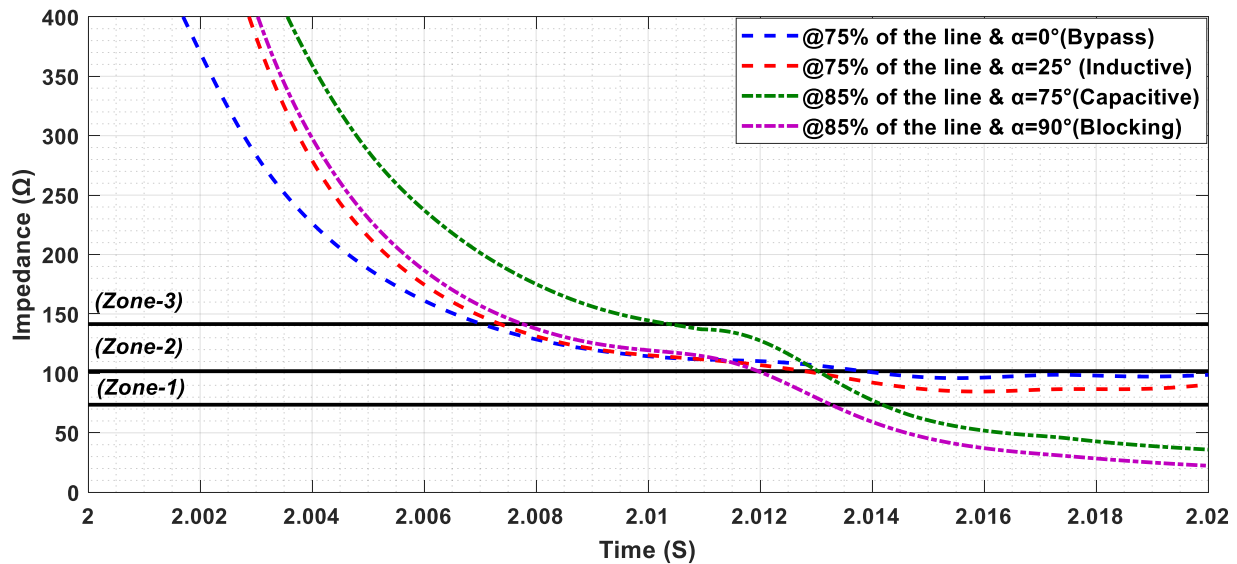


**Figure 1.** The apparent impedance under L-G faults at 2 s for different TCSC operation modes.

- For a simulated fault in zone-2 (at 85% of the protected line) and due to the TCSC impedance, the relay overreaches and detects the fault in zone-1 in both blocking mode ( $\alpha = 90^\circ$ ) and capacitive mode ( $\alpha = 75^\circ$ ).
- On the other hand, for a simulated fault in zone-1 (at 75% of the protected line) and due to the TCSC impedance, the relay underreaches and detects the fault in zone-2 in both inductive mode ( $\alpha = 25^\circ$ ) and bypass mode ( $\alpha = 0^\circ$ ).

In this study, TCSC impedance ( $X_{TCSC}$ ) modelling is applied here according to the practical design values, and the equivalent impedance will be the function of line impedance ( $Z_L$ ) and the compensation factor ( $\psi$ ), as described in [28]:

$$X_{TCSC(\alpha)} = \psi \cdot Z_L \quad (1)$$

### 3. Proposed Dynamic Quadrilateral Distance Relay

The main purpose of this article is to apply an accurate and simple solution for the problems facing distance quadrilateral relays for TCSC-compensated TLs under high resistance faults. This target can be achieved by introducing a new setting approach for both resistive and reactive reaches of quadrilateral distance relays independently. The dynamic updating of both settings will be separately controlled based on the fault resistance occurrence and including TCSC impedance in the faulted path. The proposed dynamic quadrilateral trip boundary will be described in the following subsections.

#### 3.1. Preliminary Basic Considerations

The quadrilateral distance characteristic is not a straightforward characteristic such as the Mho distance elements, as the combination of distance elements can create different shapes and polygonal characteristics. The quadrilateral characteristic is constructed, as shown in Figure 2, from the following elements [8]:

- A directional element;

- A reactance element;
- A right blinder resistance element;
- A left blinder resistance element.

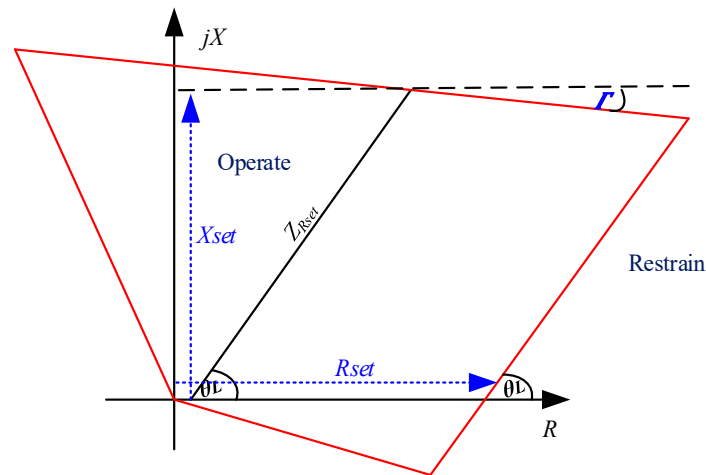


Figure 2. Quadrilateral characteristic trip boundaries.

The impedance reach of the protected line ( $Z_{Rset}$ ) is determined by the reactance element with the tilt angle ( $\Gamma$ ) declining to consider the power flow conditions during resistive faults. Moreover, the resistive fault coverage is designed by the right resistance element. The element which limits the reverse flowing load coverage is the left resistance element and a directional element keeps the faults detected in the forward direction only.

### 3.2. Adaptive Reactive Reach

Prevalent reactive setting design is achieved by considering the appropriate setting of line reactance relevant to the protected zone. To obtain the desired reactive setting ( $X_{Set}$ ) for reactance elements, the reactance line setting reach ( $X_{Rset}$ ) shall be compensated for by TCSC impedance ( $X_{TCSC(\alpha)}$ ) as follows:

$$X_{Set} = X_{Rset} \pm X_{TCSC(\alpha)} \tag{2}$$

Non-homogeneity systems affect the sensitivity of the reactance element, which will move downwards or upwards based on the power flow conditions during the asymmetrical phase or grounded resistive faults. To enhance the reactance performance for such conditions, the reactance element has to be polarized by the fault current ( $I_f$ ). However, because the fault loop current is not measurable, the current at the relay ( $I_M$ ) can be used instead of  $I_f$ . As the zero and negative sequences occur due to faults, so they are good polarizing choices. The negative sequence relay current ( $I_{M2}$ ) is used here to polarize the reactance element after adjusting the measured angle of the fault current, which is known as tilt angle ( $\Gamma$ ) [8].

For TCSC-compensated TLs, the polarized negative sequence current is altered to include the  $X_{TCSC}$  value. Therefore, the negative sequence network of the TCSC-compensated TL at the mid-point is illustrated in Figure 3.

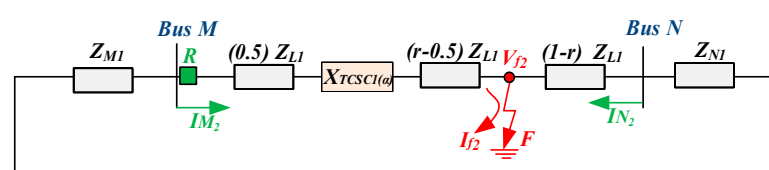


Figure 3. Two-source negative sequence network.

Considering a line-to-ground (L-G) bolted fault at the reach of zone-1 ( $r$ ) of a TL with  $Z_{L1}$  positive sequence line impedance, and where  $Z_{M1}$  and  $Z_{N1}$  are the positive sequence source impedances at both TL terminals ( $M$  and  $N$ ), the negative sequence of the fault voltage is thus described as follows:

$$V_{f2} = I_{N2} (Z_{N1} + (1 - r)Z_{L1}) \quad (3)$$

$$V_{f2} = I_{M2} (Z_{M1} + r \times Z_{L1} \pm X_{TCSC1(\alpha)}) \quad (4)$$

where “1” denotes a positive sequence while “2” denotes a negative sequence.

Knowing that  $I_{f2} = I_{M2} + I_{N2}$  and according to Equations (3) and (4), the tilt angle ( $\Gamma$ ) can be expressed by:

$$\Gamma = \arg\left(\frac{I_{f2}}{I_{M2}}\right) = \arg\left(\frac{Z_{M1} + Z_{L1} \pm X_{TCSC1(\alpha)} + Z_{N1}}{Z_{N1} + (1 - r)Z_{L1}}\right) \quad (5)$$

Note that the negative sequence impedance of the source, line and TCSC are similar to the corresponding positive sequence impedance values.

### 3.3. Adaptive Resistive Reach

The responsibility of the right resistance element in a quadrilateral distance relay is the fault resistance coverage. This component of the quadrilateral distance relay will be dynamically accommodated in the proposed scheme to detect fault resistance as much as possible, on the condition that:

- It is inherently immune in terms of selectivity, in order to operate for faults in an appropriate desirable zone;
- It is inherently immune in terms of security, in order to avoid mal-operation for external faults or load encroachment scenarios.

To perform adaptively resistive reach setting for each selective protected zone for TLs possessing TCSC compensation, a set of equations is applied based on apparent impedance calculated by the relay and circuit theory approach. An adaptive resistive blinder for ground elements is obtained by defining the fault resistance border ( $R_{fset}$ ) and the shifting resistive line setting reach ( $R_{Rset}$ ) with an  $R_{fset}$  value set by the positive sequence line impedance angle ( $\theta_L$ ).

To perform the fault zone identifier subroutine, the modified *Takagi* principle will accommodate for TCSC-compensated TLs. The modified method that uses the zero-sequence relay current ( $I_{M0}$ ), instead of the superposition current used in the Takagi method to discriminate between ground and phase faults and to consider system loading during grounded faults [29], is developed to include the TCSC impedance effect. In addition, for non-homogeneous system correction, the investigated tilt angle will be considered for fault zone identifier ( $a_Z$ ), where  $V_M$  is the voltage at terminal  $M$  that is equivalent to the relay voltage as:

$$a_Z = \frac{\text{Imag}(V_M \times (3 I_{M0})^* \times e^{-j\Gamma})}{\text{Imag}((Z_{L1} \pm X_{TCSC1(\alpha)}) \times I_M \times (3 I_{M0})^* \times e^{-j\Gamma})} \quad (6)$$

where  $a_Z \leq 0.8$  for faults in zone-1,  $a_Z \leq 1.2$  for faults in zone-2, and finally  $a_Z \leq 2.0$  for faults in zone-3.

The adaptive ground element reach setting ( $R_{Set}$ ) can be designated by the following equation, and is based on  $R_{fset}$  that is calculated after the faulted zone is identified, where  $Z_{app}$  is the impedance seen by the distance relay,

$$R_{Set} = R_{Rset} + R_{fset} \quad (7)$$

$$R_{fset} = \text{Real}(Z_{app}) - R_{Rset} \quad (8)$$

It is important to notice that the adaptive setting reach for phase elements can be achieved by shifting the resistive line reach setting ( $R_{Rset}$ ) from zero to the  $\theta_L$  angle (positive sequence line impedance angle), as the three phase elements are not accountable for any fault resistance coverage.

The flowchart, displayed in Figure 4, shows the equation flow of the resistive reach setting adaptation for the ground distance elements.

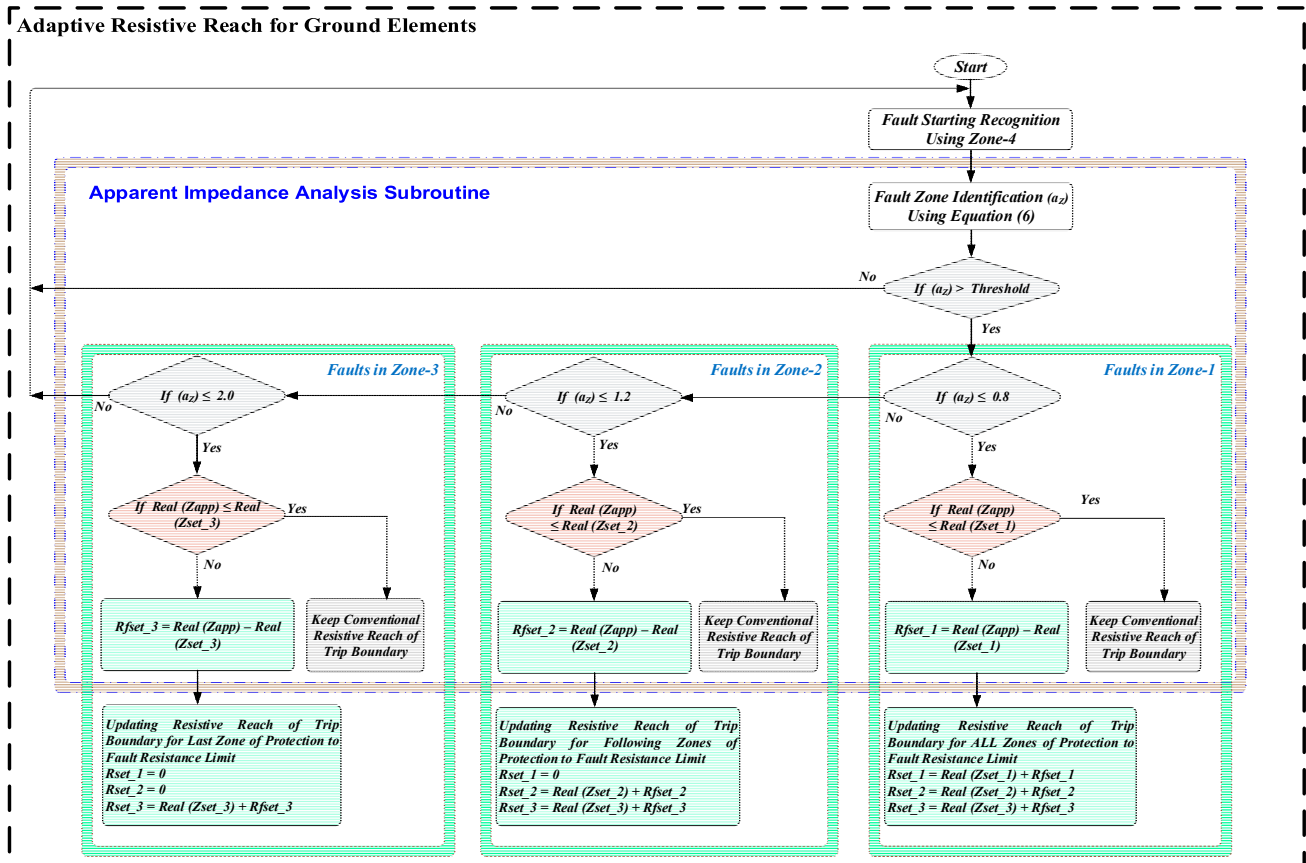


**Figure 4.** Proposed approach for adaptive resistive reaches for ground elements, Numbers 1, 2, or 3 denote zones-1,-2, or -3, respectively.

### 3.4. General Procedures of the Proposed Scheme

To reduce the burden issues on the distance relay, the proposed dynamic quadrilateral relay adapts its reactive and resistive reaches upon receiving a signal from the fault starting recognition subroutine.

The fault starting recognition can be identified by developing zone-4, which has large quadrilateral boundaries. Its resistive reach relies on the minimum load resistance equivalent to the maximum power transfer capability transmitted via the protected, compensated TL ( $P_{max}$ ) under maximum compensation during the TCSC capacitive mode ( $X_{TCSCmax\_cap}$ ).

$$P_{max} = \frac{V_M \times V_N}{Z_L - X_{TCSCmax\_cap}} \sin(\delta - \alpha_{max\_cap}) \quad (9)$$

where  $V_N$  and  $\delta$  are the receiving end voltage source and load angle, respectively, and  $\alpha_{max\_cap}$  is the firing angle under maximum compensation for the capacitive mode.

Thus, the reactive reach of zone-4 ( $X_4$ ) can be determined from the maximum expectation of the reactive reach that can occur during the TCSC inductive mode ( $X_{TCSCmax\_ind}$ ), as

$$X_4 = \text{Imag}(Z_L) + X_{TCSCmax\_ind} \quad (10)$$

The general procedures of the proposed scheme are briefly summarized in Figure 5, where:

- Two separate subroutines (based on Sections 3.2 and 3.3) will be in progress to set both the reactive and resistive reaches of the quadrilateral distance relay independently as soon as a launching signal is initiated from the fault starting recognition stage.
- TCSC zone identification stage is simply achieved as applied in [30], based on subtracting the TCSC terminal RMS current at the time of fault starting recognition from the corresponding RMS line current measured at the relay terminal.

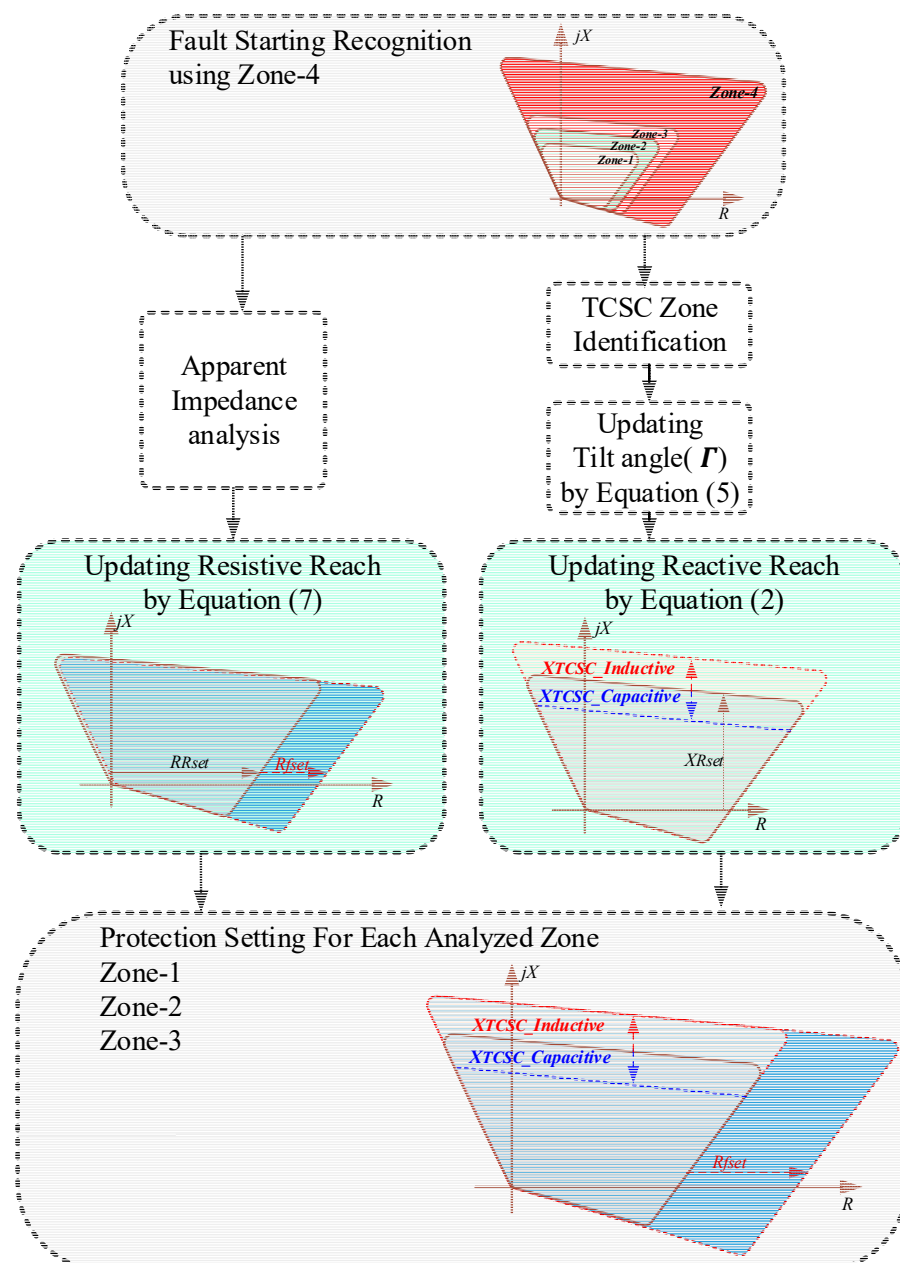


Figure 5. General procedures of the proposed scheme.

This proposed quadrilateral characteristic relay approach can be applied for any non-homogeneous system (as will be shown later in the tested systems), as well as TCSC-compensated TLs under high fault resistance. The scheme is sequential; thus, after the fault starting recognition is achieved, two separate subroutines will proceed to update both the reactive and resistive settings for each zone. Thus, the settings of zone-1 of the relay

are computed first, followed by the settings of zone-2, and then the settings of zone-3 are determined.

This approach will be applied independently for both *Ground* and *Phase* distance relay elements; the only difference between them is that the adaptation of the resistive reach in the phase element can be achieved by shifting the resistive line reach setting ( $R_{Rset}$ ) by changing the by the value of positive sequence line impedance angle ( $\theta_L$ ).

#### 4. Proposed Scheme Validation

##### 4.1. Tested Systems

The investigated methodology is tested on several faulty cases generated on TCSC-compensated TLs through the Matlab simulation program by varying the fault locations, TCSC mode, and fault resistance value on an IEEE-9 bus small power system network that has long TLs. Furthermore, the tests are repeated on an IEEE 39-bus system, as a large network system with short TLs, in order to validate and generalize the proposed scheme.

It must be pointed out that, in each of the two simulated networks, the network lines have different line parameters that significantly affect system homogeneity, in addition to the fact that the TCSC impedance will affect the protected line parameters, which have been carefully considered in the adaptive proposed scheme.

##### 4.2. Results of the IEEE-9 Bus System

As described in [30], this 60 Hz test system consists of three machines connected to a ring system of nine buses operating at 230 kV through step up transformers of 13.8 kV/230 kV. Each line section is 100 km in length. The loads are added at three locations at different buses. TCSC is connected, as shown in Figure 6, at the mid-point of the line between buses 9 and 6 while the proposed designed relay is located at bus 9. The protected zones are sequentially considered at 80% of the protected line for zone-1, while zone-2 and zone-3 are extended to 100% of the same line and 20% of the adjacent line, and 100% of the same protected line and 100% adjacent line, respectively.

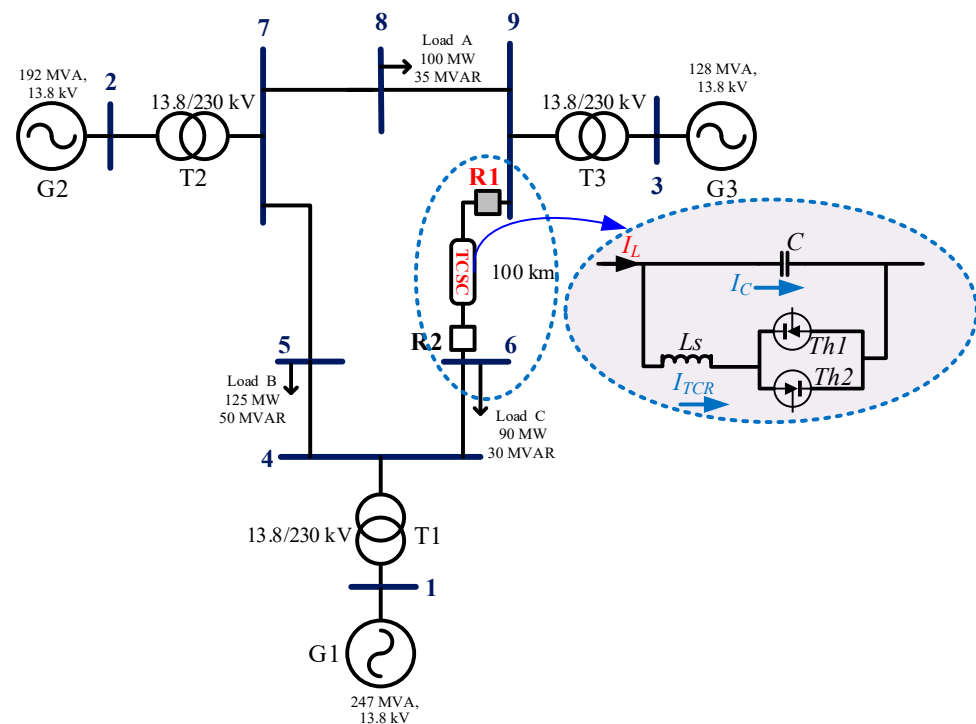


Figure 6. IEEE-9 bus system equipped with TCSC.

The evaluation divides the tests into five categories to assess the different fault scenarios and evaluate the dependability of each design setting compared with the conventional quadrilateral setting.

- Bolted faults without TCSC;
- Adaptive reactive setting while TCSC is included and without fault resistance;
- Adaptive resistive setting for faults before TCSC;
- Adaptive resistive setting for faults after TCSC;
- Evaluating the proposed scheme at the two ends of TL.

#### 4.2.1. Bolted Faults without TCSC

For selectivity and effectiveness issues, the proposed scheme is evaluated under bolted ground faults along TL at different fault locations for instantaneous and back-up zones of protection without TCSC.

The trajectory impedances of the proposed scheme (the solid black characteristic) and the conventional relay (the dashed red characteristic) are addressed in Figure 7 for the bolted L-G fault at 2.025 s under different locations on TL to cover all the zones of protection without TCSC. As shown in the figure, the proposed scheme (black) coincides with the conventional one (red) as there is no need for any adaptive reaches under plain fault conditions, which reduces the computational burden of the relay.

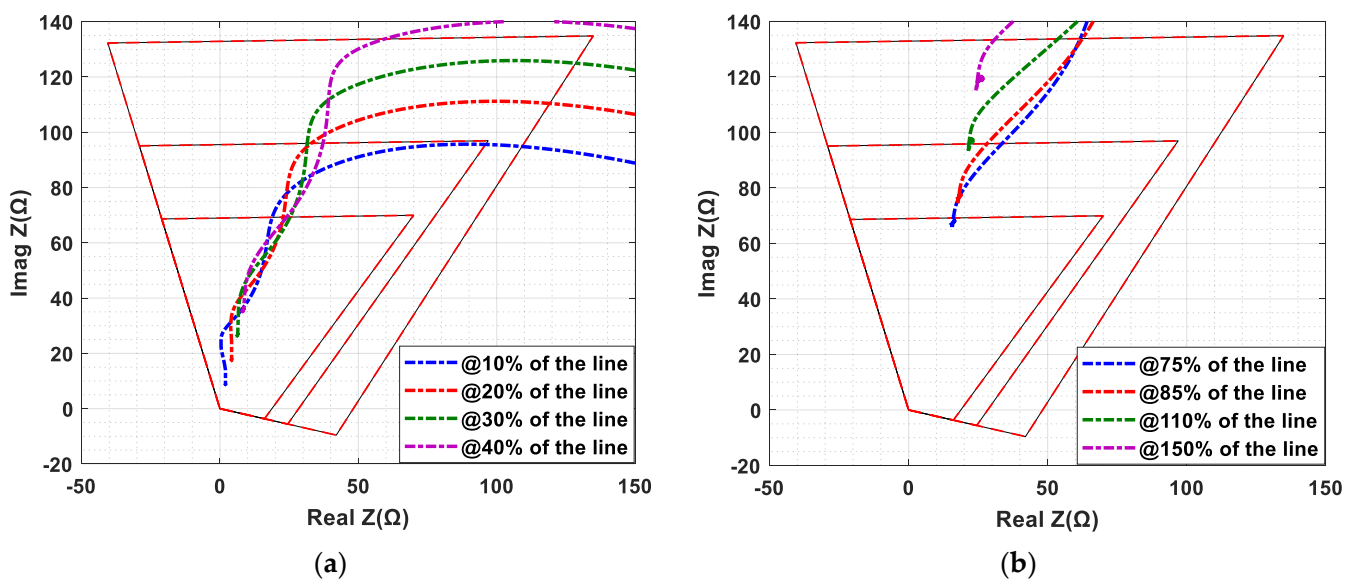


**Figure 7.** Impedance trajectory for bolted L-G faults at 2.025 s. (a) Faults before the mid-point of the protected line; (b) faults after the mid-point of the protected line.

#### 4.2.2. Adaptive Reactive Setting While TCSC Is Included and without Fault Resistance

As discussed, the adaptive reactive setting will be only applied in the case that TCSC is included in the faulted loop. Thus, for bolted faults before TCSC, the TCSC identification zone is inactivated, and therefore the adaptive scheme does not proceed. Accordingly, the settings of all zones are matched with the conventional characteristic settings (dashed red characteristic) as in case (a) of Figure 7.

To evaluate changing of the reactive setting reach adaptively, many cases of bolted ground faults are applied after TCSC under different TCSC modes of operation. The worst cases for the four modes of operation in all zones are addressed here for assessment of the scheme.

- For capacitive and blocking TCSC operation, the apparent impedance trajectory for 2L-G bolted faults at 85% and 125% of the protected line from the tested relay @is presented in Figure 8. As displayed, the conventional distance relay overreaches

in both modes of operation and detects zone-2 faults (at 85%) and zone-3 faults (at 125%) incorrectly as zone-1 faults. Meanwhile, the proposed adaptive quadrilateral distance relay (the solid black characteristic) succeeded in detecting such faults in their corresponding zones of protection by reducing the reactive reach by the TCSC reactance value.

- For the inductive and bypass modes, Figure 9 demonstrates the trajectory impedance for the bolted 3L-G fault performed at 75% and 110% of the protected line near the end edges of zone-1 and zone-2, respectively. As shown in the figure, the proposed scheme correctly detected the faults occurring in zone-1 (at 75%) and zone-2 (at 110%) for both modes of TCSC operation, while mal-operations occurred with the conventional settings that experience tricky underreaching in both cases.

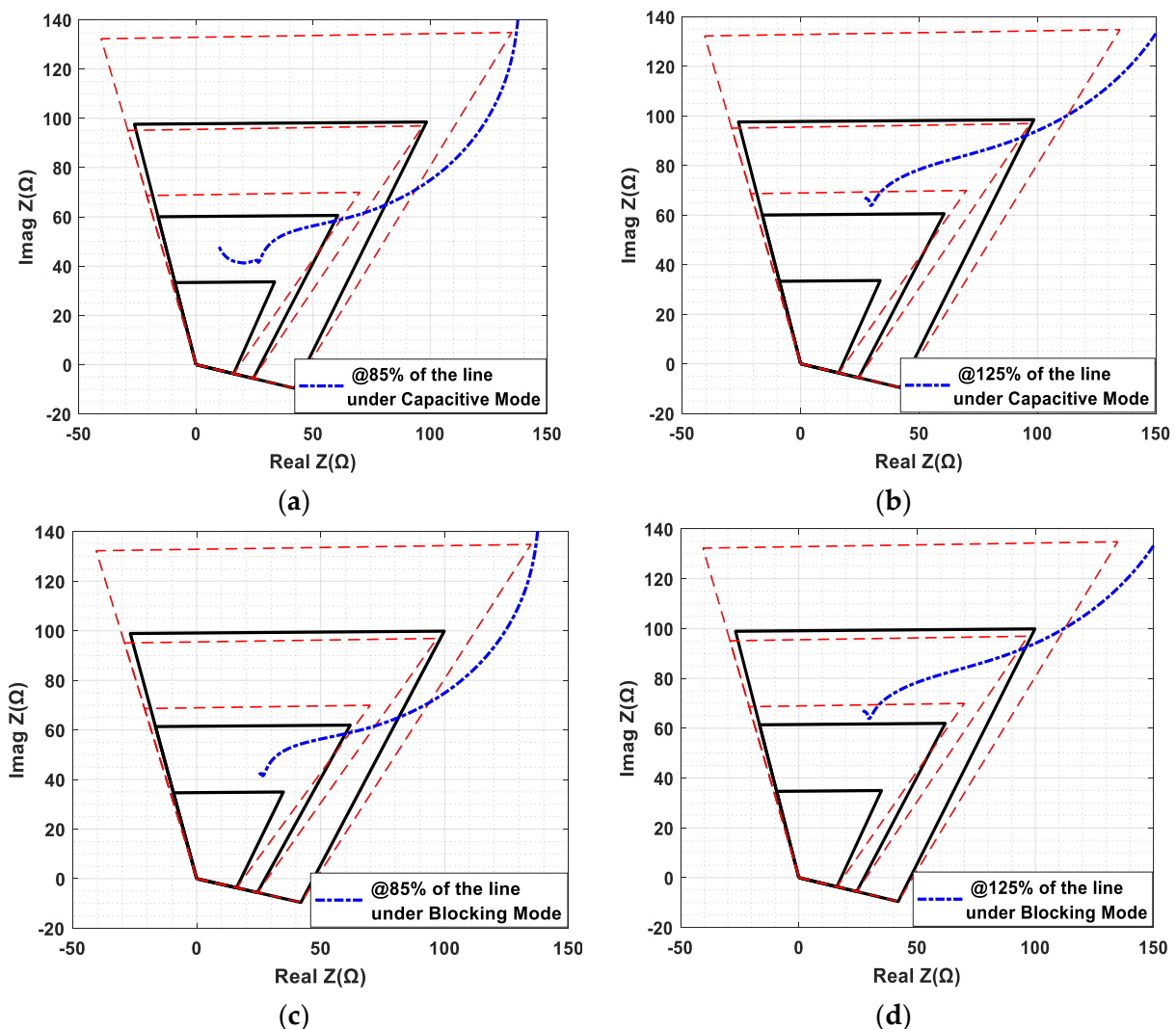


**Figure 8.** Impedance trajectory for the 2L-G fault at 2.0 s. (a) At 85% of the line under capacitive mode; (b) at 125% of the line under capacitive mode; (c) at 85% of the line under blocking mode; (d) at 125% of the line under blocking mode.

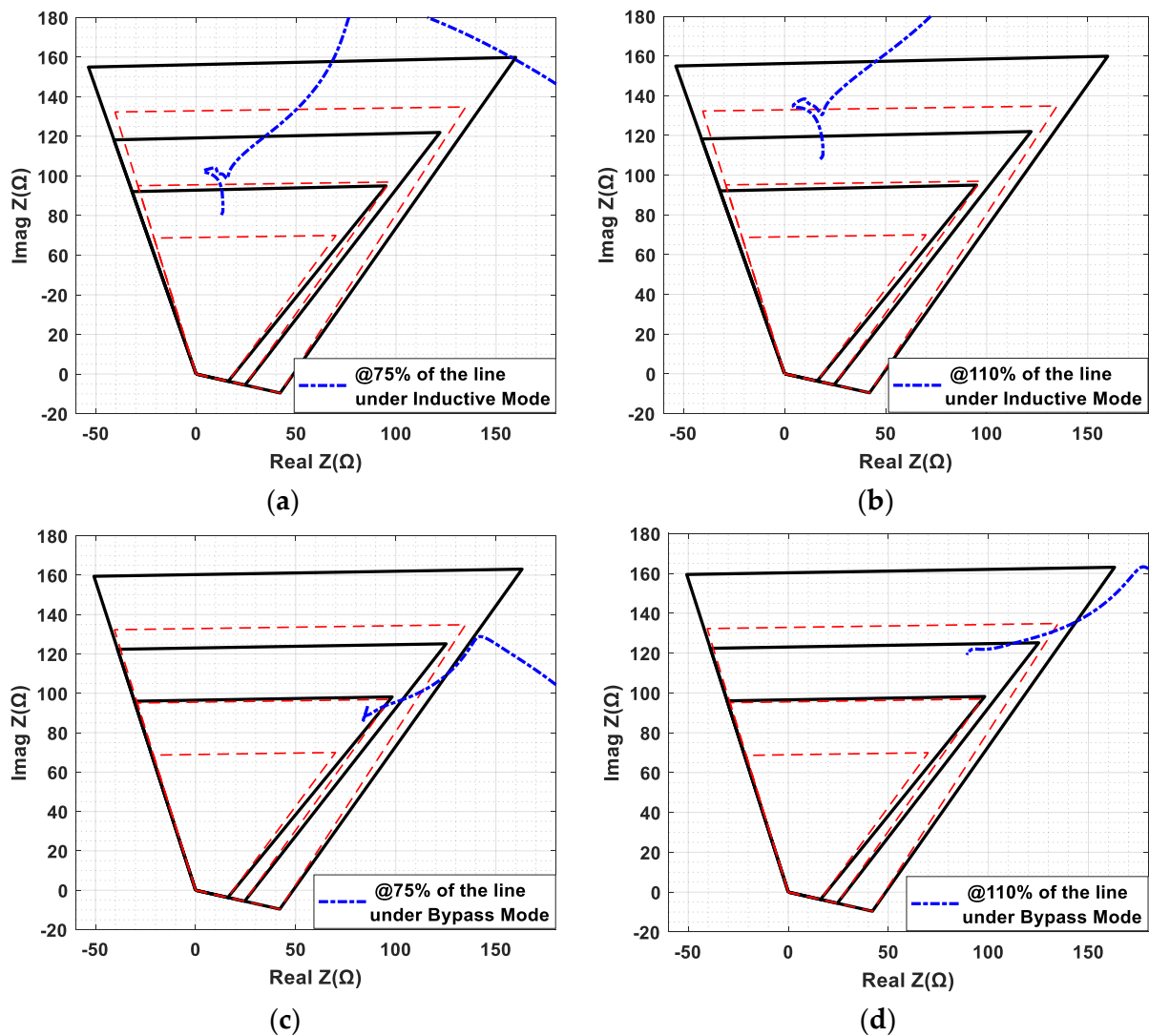


**Figure 9.** Impedance trajectory for the 3L-G fault at 2.025 s. (a) at 75% of the line under inductive mode; (b) at 110% of the line under inductive mode; (c) at 75% of the line under bypass mode; (d) at 110% of the line under bypass mode.

#### 4.2.3. Adaptive Resistive Setting for Faults before TCSC

For evaluating the effectiveness of updated resistive scheme, a set of different resistive L-G faults (with 50  $\Omega$ , 100  $\Omega$ , 200  $\Omega$ , and 250  $\Omega$  fault resistance) were implemented every 10% of the protected line before TCSC in either the capacitive or inductive mode.

As illustrated in Figure 10, the conventional relay (the dashed red characteristic) lost its selectivity for all faults with resistance 50  $\Omega$  which occurred at zone-1, and falsely detected them in zone-3. Furthermore, the conventional relay was unable to detect the remaining faults under 100  $\Omega$ , 200  $\Omega$ , and 250  $\Omega$ . On the contrary, the proposed scheme (the solid black characteristic) superiorly adapted its resistive blinder to sufficient reach based on the fault location and fault resistance value in all cases. However, TCSC is inserted in TL but, as these faults are before TCSC, the reactive reach kept its setting the same as the conventional relay.

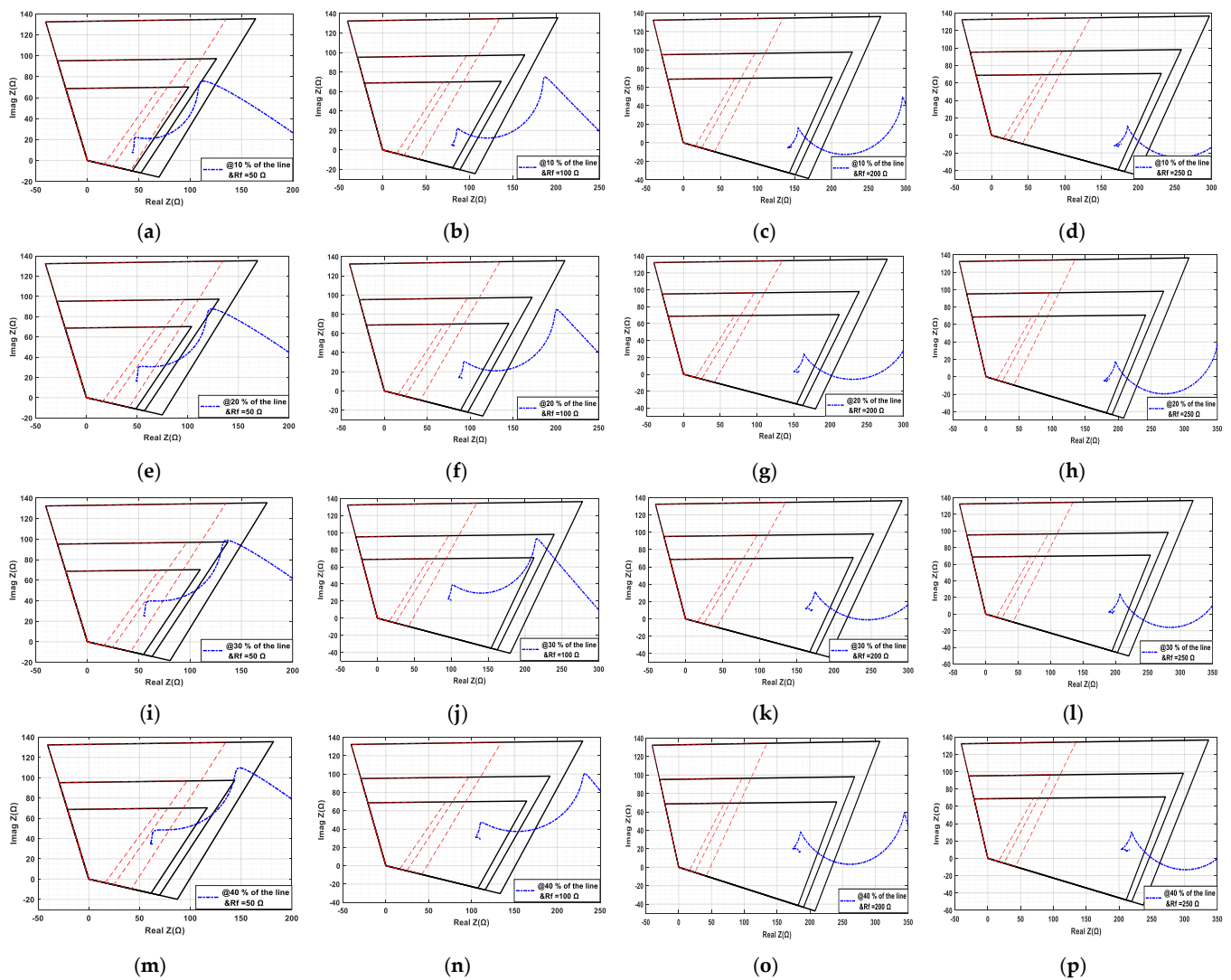


**Figure 10.** Impedance trajectory for the L-G fault at 2.025 s. (a) At 10% and  $R_f = 50 \Omega$ ; (b) at 10% and  $R_f = 100 \Omega$ ; (c) at 10% and  $R_f = 200 \Omega$ ; (d) at 10% and  $R_f = 250 \Omega$ ; (e) at 20% and  $R_f = 50 \Omega$ ; (f) at 20% and  $R_f = 100 \Omega$ ; (g) at 20% and  $R_f = 200 \Omega$ ; (h) at 20% and  $R_f = 250 \Omega$ ; (i) at 30% and  $R_f = 50 \Omega$ ; (j) at 30% and  $R_f = 100 \Omega$ ; (k) at 30% and  $R_f = 200 \Omega$ ; (l) at 30% and  $R_f = 250 \Omega$ ; (m) at 40% and  $R_f = 50 \Omega$ ; (n) at 40% and  $R_f = 100 \Omega$ ; (o) at 40% and  $R_f = 200 \Omega$ ; (p) at 40% and  $R_f = 250 \Omega$ .

As described before, the fault resistance border ( $R_{fset}$ ) is determined using Equation (8), and therefore the new updated resistive setting will be directly identified according to the fault resistance. As shown in Figure 10, when the fault occurs in zone-1 (as an instantaneous protected zone), the trip boundaries of three zones of protection will be adaptively changed by updating their resistive reach.

#### 4.2.4. Adaptive Resistive Setting for Faults after TCSC

The performance of the proposed dynamic quadrilateral relay can be compared to the conventional relay with fixed characteristic settings by applying a set of resistive faults after TCSC under the four different modes of operation at different critical locations, where the conventional relay may lose its selectivity-relaying function by underreaching/overreaching significantly due to the existence of TCSC reactance in the faulted loop.

Figures 11–14 illustrate the correctness of the dynamically updated settings (the solid black characteristic) for L-G faults at 2.025 s with  $R_f = 50 \Omega$ ,  $100 \Omega$ , and  $200 \Omega$  at locations 85% and 125% under the blocking mode and capacitive TCSC modes, respectively. In addition, the same faults are simulated with similar fault conditions but at 75% and 110% of the line under the inductive and bypass TCSC modes of operation, respectively.

On contrary, the conventional fixed characteristic settings (the dashed red characteristic) completely failed to detect such faults due to both the effects of fault resistance and the existence of TCSC in the fault loop.

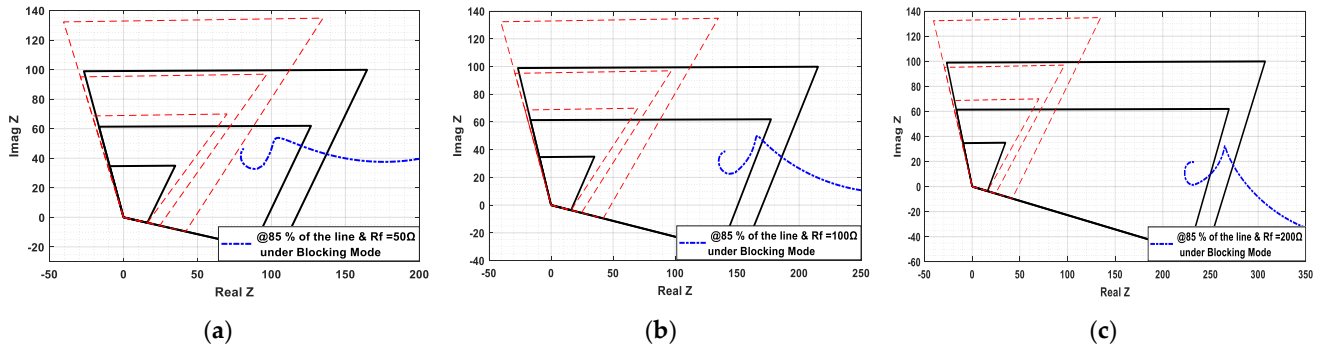


**Figure 11.** Apparent impedance locus for the L-G fault at 2.025 s at 85% of the line under the TCSC blocking mode. (a) With  $R_f = 50 \Omega$ ; (b) with  $R_f = 100 \Omega$ ; (c) with  $R_f = 200 \Omega$ .

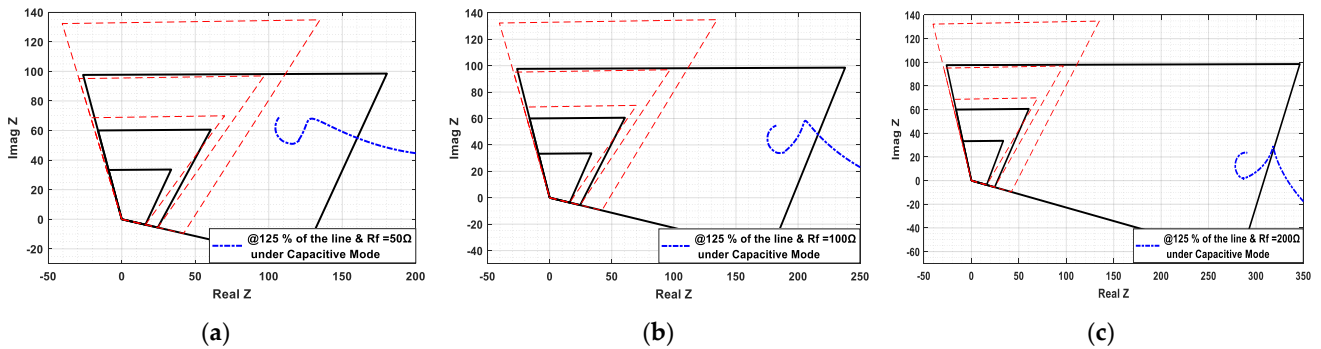


**Figure 12.** Apparent impedance locus for the L-G fault at 2.025 s at 125% of the line under the TCSC capacitive mode. (a) With  $R_f = 50 \Omega$ ; (b) with  $R_f = 100 \Omega$ ; (c) with  $R_f = 200 \Omega$ .

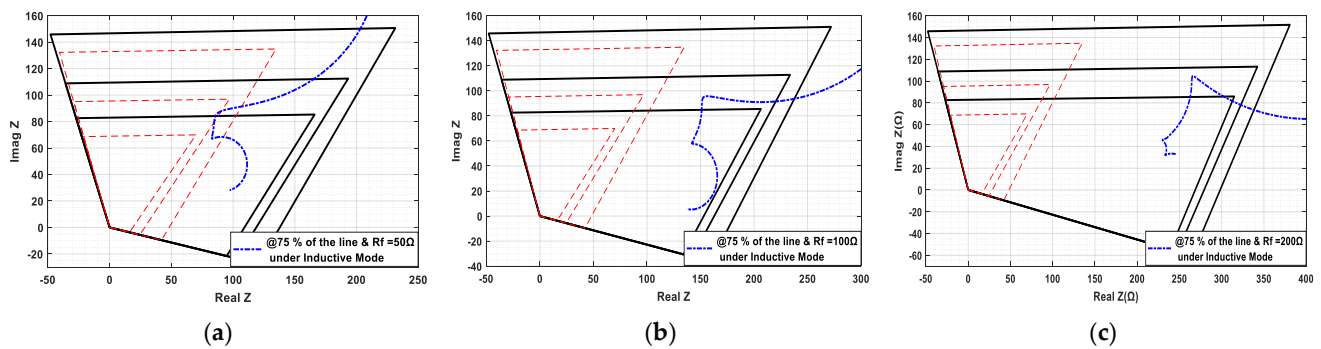


**Figure 13.** Apparent impedance locus for the L-G fault at 2.025 s at 75% of the line under the TCSC inductive mode. (a) With  $R_f = 50 \Omega$ ; (b) with  $R_f = 100 \Omega$ ; (c) with  $R_f = 200 \Omega$ .

It is also worth clarifying here that the scenario of the resistive faults with TCSC included in the faulted loop is different from the cases for faults without TCSC. Although TCSC has only inductance behaviour, but it affects the resistive reach unless its negative impact is compensated for by tile angle, as discussed in Equation (5) and considered in the fault zone identifier by modifying the Takagi method in Equation (6) to determine the fault resistance border. Otherwise, the  $R_f$  term will be a complex value and adds an additional reactance value to the fault. Additionally, if the proposed adaptive dynamic setting scheme only adapts the resistive reach without adapting the reactive reach, the relay will falsely detect the resistive fault due to underreach or overreach depending on TCSC operational

mode. Accordingly, it is concluded that the proposed dynamic setting scheme is essential for such cases.

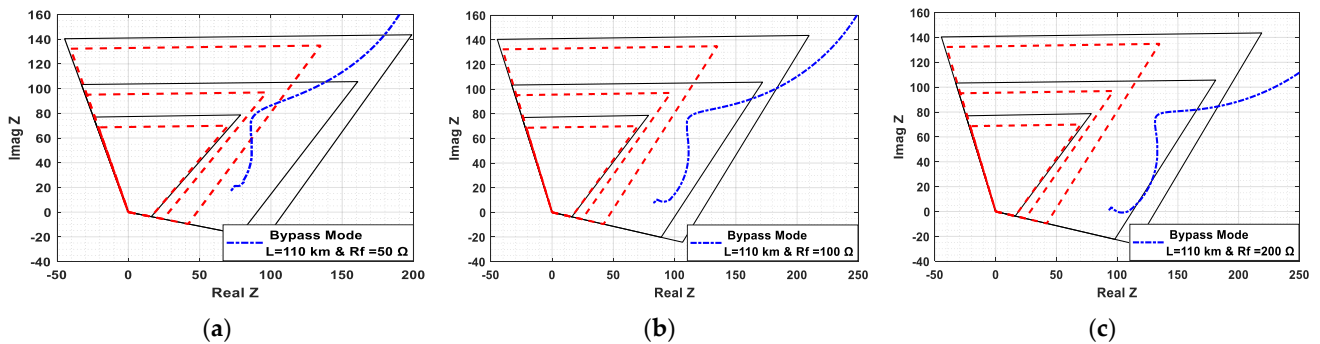


**Figure 14.** Apparent impedance locus for the L-G fault at 2.025 s at 110% of the line under the TCSC bypass mode. (a) With  $R_f = 50 \Omega$ ; (b) with  $R_f = 100 \Omega$ ; (c) with  $R_f = 200 \Omega$ .

#### 4.2.5. Evaluating the Proposed Scheme at the Two Ends of TL

An L-G fault is simulated under the capacitive TCSC mode at 2.015 s with a large  $R_f$  of  $150 \Omega$  at the location of 85% from the first relay R1 (in its zone-2), which also means that the fault is 15% from the opposite relay R2 (in its zone-1).

Upon implementing the proposed scheme in both relays (R1 and R2), Figure 15 illustrates the effectiveness of their dynamically updated settings (black solid) compared with the conventional characteristic settings (red dashed) which failed to detect this fault from both ends.

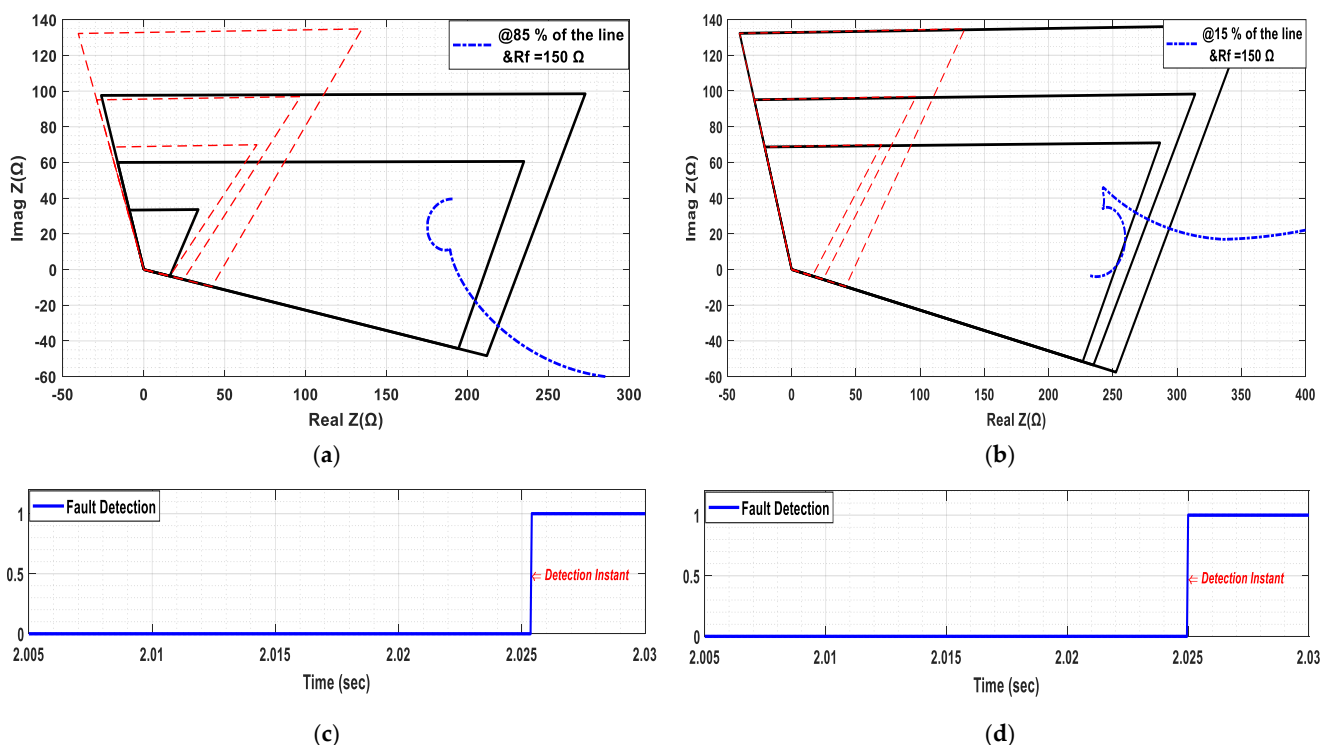


**Figure 15.** An L-G fault under the capacitive TCSC mode at 2.015 s with  $R_f = 150 \Omega$  at the location of 85% from the first relay R1. (a) Characteristics of the first end relay R1; (b) characteristics of the second end relay R2; (c) fault detection of the first end relay R1; (d) fault detection of the second end relay R2.

As is clearly shown, the proposed dynamic relay R1 correctly detected the fault in its zone-2 (detected it at 2.0254 s) by adapting both resistive and reactive reach so its tripping time was delayed by the zone-2 time delay, while the proposed dynamic relay at

R2 succeeded in detecting the same fault in its zone-1 (detecting it at 2.025 s) by adapting only its resistive reach without adapting its reactive reach, as TCSC is not included in its faulted path and thus it trips instantaneously.

#### 4.3. Further Evaluation on a Larger Test System—IEEE-39 Bus System

In order to validate the proposed scheme on a larger test system, the methodology was widely examined on the modified 60 Hz IEEE-39 bus New England system, as shown in Figure 16 [31]. In the modified 39-bus system, TCSC is placed at the mid-point of the line between buses 28 and 29.

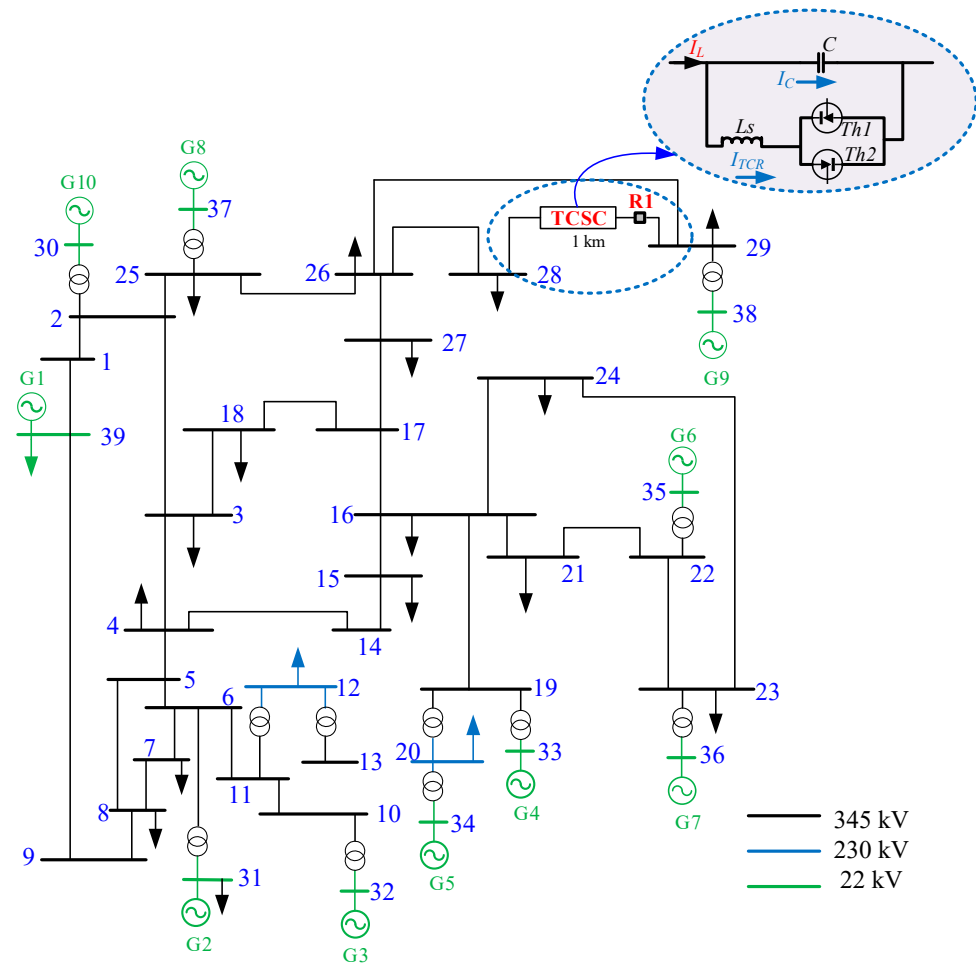


**Figure 16.** Schematic diagram of the IEEE 39-bus New England system compensated for by TCSC.

It is to be noted that the TCSC compensation provided in the 39-bus test system is exactly the same as that discussed for the IEEE-9 bus power system in the earlier section. The proposed distance relay R1, placed at bus-29 for protecting lines 28–29, is considered for performance evaluation. A set of resistive grounded faults are applied on different locations, after the TCSC location, in both the capacitive and inductive modes of operation, with different fault resistance, to evaluate the proposed relay performance and dynamically updating the resistive and reactive reaches under either the capacitive or inductive TCSC modes of operation.

Figure 17 demonstrates the trajectory impedance for L-G faults at the end of zone-1 of the tested relay (at 75%) with  $R_f = 50 \Omega$  and  $100 \Omega$ , and also at the end of zone-2 (at 110%) with  $R_f = 50 \Omega$  under the TCSC inductive mode. The figure highlights the performance of the proposed relay with dynamically updated settings (the solid black characteristic) versus the conventional relay with the fixed characteristic (the dashed red characteristic). The achieved results confirmed the success of the proposed scheme in detecting all faults

with a high degree of selectivity. As is clearly shown, the faults at 75% are detected correctly in zone-1, either with 50  $\Omega$  fault resistance (case-a) or 100  $\Omega$  fault resistance (case-b); in addition, the fault at 110% of the line is detected properly in zone-2 (case-c) due to the zone identification method, while the fixed conventional setting completely failed to detect such faults.

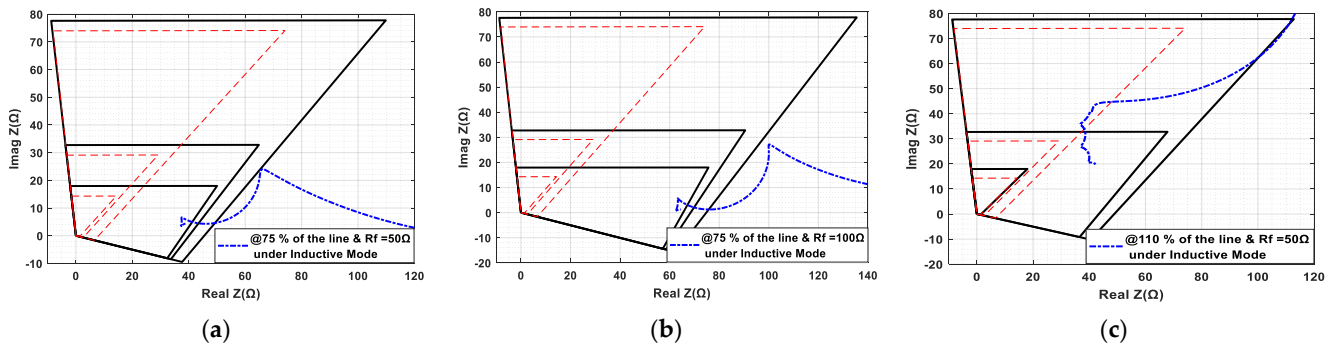


**Figure 17.** Apparent impedance for the L-G fault at 1.0 s under the TCSC inductive mode. (a) At 75% and  $R_f = 50 \Omega$ ; (b) at 75% and  $R_f = 100 \Omega$ ; (c) at 110% and  $R_f = 50 \Omega$ .

Under the TCSC capacitive mode, the impedance trajectory for 2L-G faults in zone-2 and zone-3 is illustrated in Figure 18. For cases a and b, the faults occurred at 85% of the line with  $R_f = 50 \Omega$  and  $100 \Omega$ , while in case c, the fault was simulated at the beginning of zone-3 (at 125%) with  $R_f = 50 \Omega$ . As is obviously revealed, the conventional relay lost its selectivity in all examined cases. In fact, the conventional relay erroneously underreaches in case a as the fault is detected in zone-3 and, on the other hand, it incorrectly overreaches for the fault in zone-3 as illustrated in case c. In addition, it failed to detect the fault in case b under the high fault resistance value; on the contrary, the proposed relay tripped correctly (the solid characteristic) in this case.

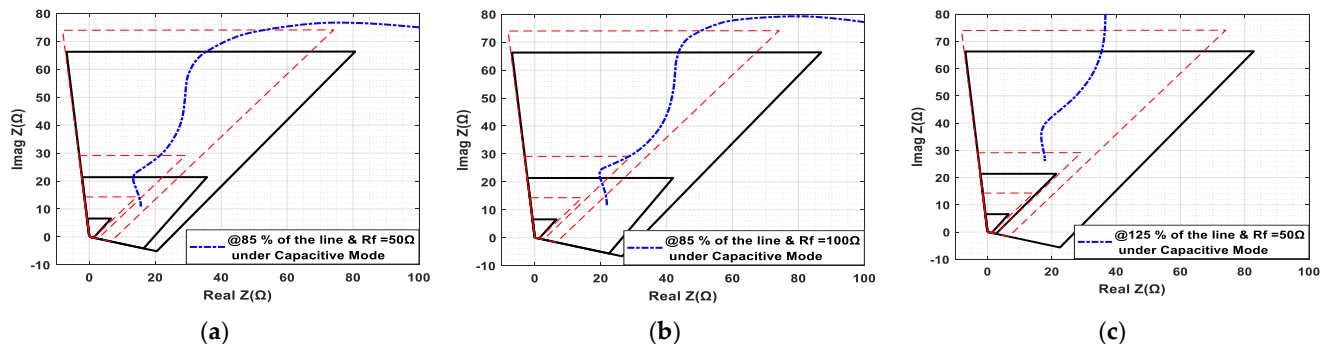


**Figure 18.** Apparent impedance for the 2L-G fault at 1.0 s under the TCSC capacitive mode. (a) At 85% and  $R_f = 50 \Omega$ ; (b) at 85% and  $R_f = 100 \Omega$ ; (c) at 125% and  $R_f = 50 \Omega$ .

As a matter of fact, the achieved results ensure the correct operation of the proposed scheme, in which the relay adapted its trip boundaries itself in the respective zones under TCSC operation, according to the local information at the relay and the received information from the TCSC terminal during faulty system conditions that the conventional relay is incapable of handling.

## 5. Features Assessment with Reference to Other Techniques

Multi-fold advantages of the proposed scheme compared to some other published techniques shall be addressed and discussed in the following section. The key advantages of the proposed scheme are addressed in terms of *Fault Detection Time*, *Fault Resistance Coverage*, and *Data Acquisition and Computation Technique*.

### 5.1. Fault Detection Time

As the proposed scheme is used for fault detection in TCSC-compensated TLs, the performance speed is critically important. Thus, assessing this approach for the fault detection time should be evaluated by investigating the detection time for one of the worst cases in zone-1 on the IEEE-9 bus system. This case occurred when L-G fault was applied at 75% of the protected line at 2.0075 s, which is implemented at the instant of zero crossing voltage with  $R_f = 200 \Omega$  under the TCSC inductive mode. As is revealed in Figure 19a, due to the high resistance fault, the current increases and the voltage decreases insignificantly and, therefore, it is expected that the conventional fixed setting will underreach for this fault. On the other hand, Figure 19b validates the timing of different stages of the proposed distance relay, starting from the fault inception time to the detection time. As is demonstrated, while the fault inception occurred at 2.0075 s, the proposed relay correctly recognised that a fault had started at 2.0166 s, and the identification of TCSC zone was achieved at 2.018 s, while the fault zone was properly identified at zone-1 at the 2.02105 s timepoint and finally the fault was detected for the correct trip at 2.02355 s, which means that only 0.01605 s was required (0.963 cycle) from the time of fault inception.

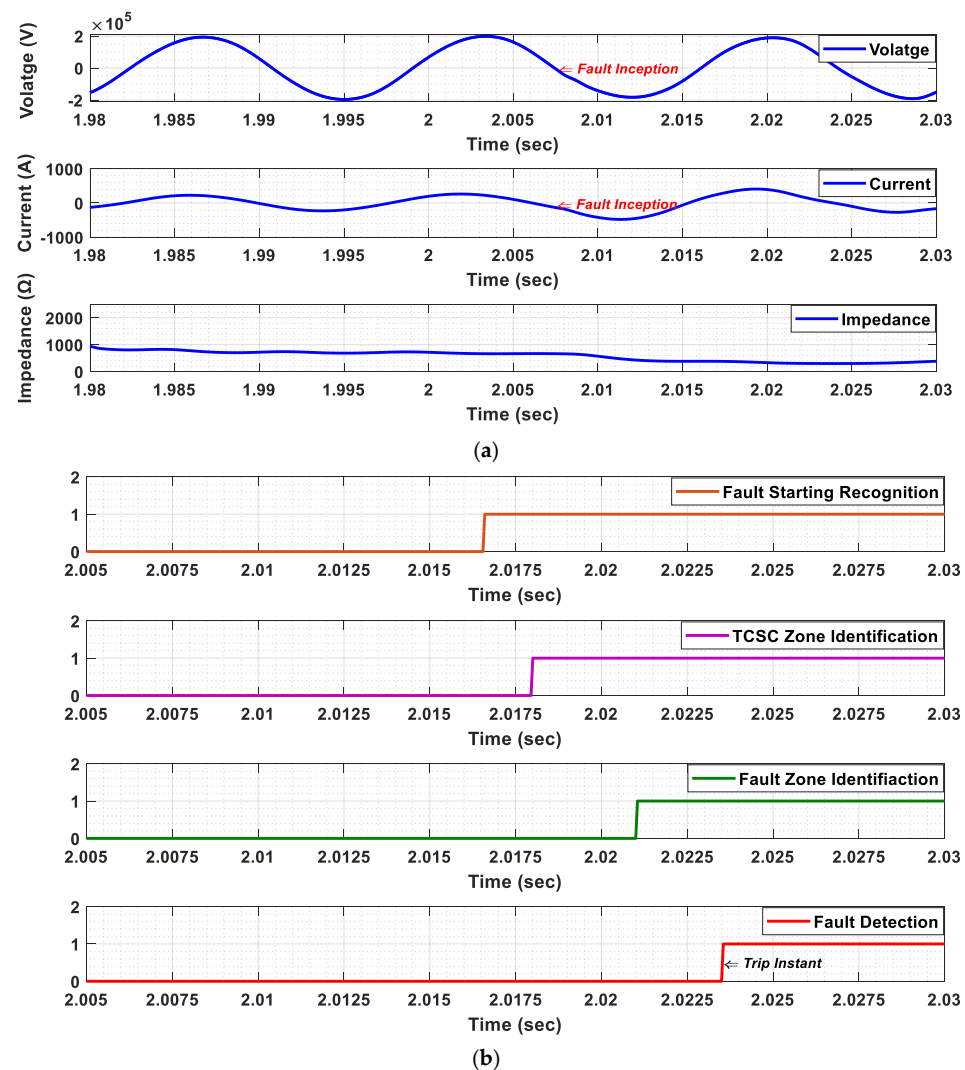


**Figure 19.** One of the worst cases in zone-1 where the L-G fault is simulated at 75% of the line at 2.0075 s. (a) Measured voltage, current at relay terminal and calculated apparent impedance; (b) timing of different stages of the proposed scheme.

Besides, the detection time is evaluated for other simulated faults occurring during capacitive TCSC cases and under high resistance faults of  $200\ \Omega$  (demonstrated in Figures 11c and 12c). It is found that all these faults are detected within less than one cycle from fault inception (about 0.75 cycle).

It is worth mentioning that this detection time is estimated for simulated cases but in real cases it may be longer. In fact, the fault detection time was affected by the *Transducer* delay that is used for voltage and current measurements, the *Processing* time that is required for converting measured data into phasor information using DFT, and the *Communication* delay that depends on the type of communication links as well as, the physical distance between the TCSC substation and relay. Therefore, for the locality of TCSC in the opposite end of the relay, the fault detection time may be affected by the communication latency. However, due the significant and continuous development of communication applications with high data rates, the 4G wireless broadband becomes 10 times faster than 3G, which helps in achieving reliable and fast protection schemes as the 4G latency is estimated as 50 ms [32]. In the near future, 5G will provide a maximal platform for different grid applications including ultra time-critical applications such as protection schemes [33].

Regarding the comparative study with other published techniques, it is worth mentioning that only the scheme introduced in [10] is faster than the proposed scheme but is so under less fault-resistance coverage. Moreover, the scheme in [10] does not consider the homogeneity system concerns that may affect the accuracy of its results in such cases.

### 5.2. Fault Resistance Coverage

According to the obtained results, the large coverage of the trip boundary of the proposed method due to the fault resistance can be clearly observed. This significant advantage is due to the development of the modified Takagi method that helps in estimating the fault zone. Therefore, the fault resistance border can be updated properly. As is discussed in the results, the fault resistance can be covered up to  $250\ \Omega$  in zone-1 and  $200\ \Omega$  in the back-up zones of protection. Although the optimization method used in [15] introduces good coverage of the resistive fault up to  $200\ \Omega$  in zone-1, the method is only applicable for the first zone and the fault is detected after a relatively long iteration time, as is habitual for optimization methods.

### 5.3. Data Acquisition and Computation Technique

As described, the proposed technique basically relies on the local data estimated at the relay terminal and only two values are received from the TCSC substation which are: the TCSC fault RMS current, to simply inform whether TCSC is included in the faulted loop or not, and the firing angle that is used in estimating the TCSC impedance. However, some reported schemes, such as those in [10] and [15], are designed based upon the local terminal data but they have some limitations, as discussed in Sections 5.1 and 5.2. In addition, in [22] and [23], the local data are utilized to reduce zone-1 setting and delayed zone-2, but [22] did not consider the fault resistance in the evaluation, rather than [23], which is just suggested based on a poor modelling of TCSC that negatively affects the accuracy of its results.

### 5.4. Comprehensive Comparative in Terms of Main Features

Table 2 summarizes the comparative study undertaken to highlight the performance of the proposed method compared with some other techniques used for quadrilateral relay settings. Therefore, the salient features of the proposed dynamic quadrilateral characteristic-based adaptive distance relay can be summarized as follows:

*Controllability:* the reactive and resistive reach can be controlled separately and independently. The reactive reach is changed considering the TCSC reactance effect and the system homogeneity effect, while the resistance is changed considering the fault resistance effect.

*Reliability*, as the selectivity feature is obtained by compensating the undesirable effect of TCSC and fault resistance. Furthermore, the security is obtained by avoiding mal-operation for any external faults.

*Economy*, as there is no need for multi-filtration devices with high level of sampling time and no synchronized data or excessive communications are required to transmit the data from the remote end.

*Inclusivity*, as the proposed method can be generalized and applied for any interconnected long or short TL.

*Ease of application*, as the method can be applied on the conventional distance relays by modifying the existing algorithm.

**Table 2.** Comparison between the proposed dynamic relay and some other methods.

Reference	Fault Detection Time	Fault Resistance Coverage	Data Acquisition	Computation Technique
[10]	—	Up to 98 $\Omega$ in zone-1	Two-terminal data	Communication added scheme
[10]	Within 0.67 cycles without compensation	Up to 50 $\Omega$ in zone-1 Up to 20 $\Omega$ in zone-2	Local data	High level of filtration
[15]	Within 1.2 s	Up to 200 $\Omega$ in zone-1	Local data	Optimization
[16]	Within 1.2 cycles	Up to 80 $\Omega$ in zone-1	Two-terminal data	Optimization
[20]	—	Up to 150 $\Omega$ in zone-1	Two-terminal data	Synchronized data scheme
[22]	Within 1 cycle	—	Local data	Reducing zone-1 setting
[23]	Within 3 cycles	Up to 95 $\Omega$ zone-1	Local data	Reducing zone-1 setting
Proposed Scheme	Within 0.75 cycles and 0.963 cycles for the worst case	Up to 250 $\Omega$ in zone-1 Up to 200 $\Omega$ in zone-2 Up to 100 $\Omega$ in zone-3	Local data	Apparent resistance and circuit theorem approach

The symbol “—” refers to information not mentioned.

## 6. Conclusions

The paper introduces a dynamic quadrilateral characteristic-based adaptive distance relay for TCSC-compensated TLs. The proposed relay adapts both the reactive reach and resistive reach independently. The reactive reach is adjusted by identifying the presence of TCSC in the faulted loop to compensate for its effect. Additionally, the calculation of the tilt angle is investigated to consider the homogeneity of the system due to the load flow and TCSC effect during high resistance faults. The resistive reach is modified adaptively in TCSC TLs by estimating the faulted zone through the modified Takagi method.

In order to validate and generalize the proposed dynamic distance relay, it is extensively tested on two simulated IEEE benchmark networks using Matlab, which are the IEEE-9 bus and New England IEEE-39 bus, to consider both a small grid with long TLs and a large network with short TLs. The proposed relay is tested on different locations to cover three zones of protection, different fault resistance values, and different TCSC modes of operation. According to the obtained results, it can be deduced that the proposed scheme has conventional functions under normal fault conditions without any burden on the relay; in addition, it is capable of detecting high resistance faults during the TCSC inductive and capacitive modes. Additionally, it can alleviate the negative impact of TCSC underreach/overreach by adapting the reactive setting. Finally, Controllability, Reliability, Economy, Inclusivity, and Ease of application are considered the salient features of the proposed dynamic quadrilateral characteristic-based adaptive distance relay.

However, if the system is subject to transient instability such as unstable power swing, the proposed method should be modified to also consider power swing tripping and blocking issues based on faults conditions. In addition, validation through real world data

will be valuable to ensure the leverage of the proposed scheme. Therefore, these issues will be studied in future publications.

**Author Contributions:** Conceptualization, D.K.I., E.A.Z.; methodology, G.M.A.-H. and D.K.I.; software, G.M.A.-H.; investigation, G.M.A.-H.; writing—original draft preparation, G.M.A.-H. and D.K.I.; writing—review and editing, D.K.I., E.A.Z., A.F.Z.; supervision, E.A.Z., A.F.Z. All authors have read and agreed to the published version of the manuscript.

**Funding:** This research received no external funding.

**Conflicts of Interest:** The authors declare no conflict of interest.

## References

- Bakshi, U.A.; Bakshi, M.V. *Protection and Switchgear*; Technical Publications Pune: Maharashtra, India, 2008.
- Joe, M.; Jackie, P. Application Guidelines for Ground Fault Protection. In Proceedings of the 1998 International Conference Modern Trends in the Protection Schemes of Electric Power Apparatus and Systems, New Delhi, India, 28–30 October 1998.
- Sauvik, B.; Paresh, K.N. State-Of-The-Art on The Protection of FACTS Compensated High-Voltage Transmission Lines: A review. *IET CEPRI* **2018**, *3*, 21–30.
- Mathur, R.M.; Rajiv, K.V. *Thyristor-Based FACTS Controllers for Electrical Transmission Systems*; John Wiley & Sons: Hoboken, NJ, USA, 2011.
- Ahad, K.; Shahram, J.; Hossein, S. Distance Relay Over-Reaching in Presence of TCSC on Next Line Considering MOV Operation. In Proceedings of the 45th International Universities Power Engineering Conference UPEC2010, Cardiff, UK, 31 August–3 September 2010.
- Beleed, H.; Johnson, B.K.; Hess, H.L. An Examination of the Impact of D-FACTS on the Dynamic Behavior of Mho and Quadrilateral Ground Distance Elements. In Proceedings of the 2020 IEEE Power & Energy Society Innovative Smart Grid Technologies Conference (ISGT), Washington, DC, USA, 17–20 February 2020; pp. 1–5. [[CrossRef](#)]
- Holbach, J.; Vadlamani, V.; Lu, Y. Issues and Solutions in Setting a Quadrilateral Distance Characteristic. In Proceedings of the 2008 61st Annual Conference for Protective Relay Engineers, College Station, TX, USA, 1–3 April 2008; pp. 89–104. [[CrossRef](#)]
- Fernando, C.; Armando, G.; Gabriel, B. *Adaptive Phase and Ground Quadrilateral Distance Elements*; Schweitzer Engineering Laboratories, Inc.: Pullman, WA, USA, 2017.
- Bogdan, K. Settings Considerations for Distance Elements in Line Protection Applications. In Proceedings of the 2021 Texas A&M Conference for Protective Relay, Presented at the 74th Annual Georgia Tech Protective Relaying Conference, College Station, TX, USA, 28–30 April 2021.
- Shateri, H.; Jamali, S. Robustness of communication aided distance relay with Quadrilateral characteristic against inter phase fault resistance. In Proceedings of the 2010 International Conference on Power System Technology, Hangzhou, China, 24–28 October 2010; pp. 1–8. [[CrossRef](#)]
- Patel, U.J.; Chothani, N.G.; Bhatt, P. Adaptive quadrilateral distance relaying scheme for fault impedance compensation. *Electr. Control. Commun. Eng.* **2018**, *14*, 58–70. [[CrossRef](#)]
- Aneesh, S.; Angel, T.S. Quadrilateral Relay Based Distance Protection Scheme for Transmission Lines under Varying System Conditions. In Proceedings of the 2015 IEEE International Conference on Technological Advancements in Power & Energy, Kollam, India, 24–26 June 2015. [[CrossRef](#)]
- Venkatanagaraju, K.; Biswal, M.; Bansal, R. Adaptive distance relay algorithm to detect and discriminate third zone faults from system stressed conditions. *Int. J. Electr. Power Energy Syst.* **2021**, *125*, 106497. [[CrossRef](#)]
- Sorrentino, E.; De Andrade, V. Optimal-Probabilistic Method to Compute the Reach Settings of Distance Relays. *IEEE Trans. Power Deliv.* **2011**, *26*, 1522–1529. [[CrossRef](#)]
- Davydova, N.; Shchetinin, D.; Hug, G.; Davydova, N. Optimization of First Zone Boundary of Adaptive Distance Protection for Flexible Transmission Lines. In Proceedings of the 2018 Power Systems Computation Conference (PSCC), Dublin, Ireland, 11–15 June 2018. [[CrossRef](#)]
- Shukla, S.K.; Koley, E.; Ghosh, S. A Novel Approach Based on Line Inequality Concept and Sine–Cosine Algorithm for Estimating Optimal Reach Setting of Quadrilateral Relays. *Arab. J. Sci. Eng.* **2020**, *45*, 1499–1511. [[CrossRef](#)]
- Serna, J.D.J.J.; López-Lezama, J.M. Calculation of Distance Protection Settings in Mutually Coupled Transmission Lines: A Comparative Analysis. *Energies* **2019**, *12*, 1290. [[CrossRef](#)]
- Orosz, T.; Rassólkin, A.; Kallaste, A.; Arsénio, P.; Pánek, D.; Kaska, J.; Karban, P. Robust Design Optimization and Emerging Technologies for Electrical Machines: Challenges and Open Problems. *Appl. Sci.* **2020**, *10*, 6653. [[CrossRef](#)]
- Srivani, S.; Vittal, K.P. Adaptive distance relaying scheme in series compensated transmission lines. In Proceedings of the 2010 Joint International Conference on Power Electronics, Drives and Energy Systems & 2010 Power India, New Delhi, India, 20–23 December 2010; pp. 1–7.
- Biswal, M.; Pati, B.B.; Pradhan, A.K. Adaptive distance relay setting for series compensated line. *Int. J. Electr. Power Energy Syst.* **2013**, *52*, 198–206. [[CrossRef](#)]

21. Achary, K.S.K.; Raja, P. Adaptive design of distance relay for series compensated transmission line. *Energy Procedia* **2017**, *117*, 527–534. [[CrossRef](#)]
22. Magagula, X.G.; Nicolae, D.V.; Yusuff, A.A. The performance of distance protection relay on series compensated line under fault conditions. In Proceedings of the AFRICON 2015, Addis Ababa, Ethiopia, 14–17 September 2015; pp. 1–6. [[CrossRef](#)]
23. Paladhi, S.; Pradhan, A.K. Adaptive Zone-1 Setting Following Structural and Operational Changes in Power System. *IEEE Trans. Power Deliv.* **2017**, *33*, 560–569. [[CrossRef](#)]
24. Seo, W.-S.; Kang, S.-H.; Yoon, Y.-D.; Yoon, J.-S. A Conventional Distance Protection for Series-Compensated Lines Considering TCSC Protected by a Metal Oxide Varistor. In Proceedings of the 2019 IEEE 8th International Conference on Advanced Power System Automation and Protection (APAP), Xi'an, China, 21–24 October 2019.
25. Woo, S.S.; Min, S.K.; Sang, H.K.; Jong, S.Y.; Chang, H.H. An Improved Setting Method of the Distance Protective LEDs for Series-Compensated Transmission Lines Based on A Case Study Approach. *Electr. Power Syst. Res.* **2020**, *188*, 106554.
26. Vyas, B.; Maheshwari, R.P.; Das, B. Protection of series compensated transmission line: Issues and state of art. *Electr. Power Syst. Res.* **2014**, *107*, 93–108. [[CrossRef](#)]
27. Ordóñez, C.; Gómez-Expósito, A.; Maza-Ortega, J. Series Compensation of Transmission Systems: A Literature Survey. *Energies* **2021**, *14*, 1717. [[CrossRef](#)]
28. Ibrahim, D.K.; Abo-Hamad, G.M.; Zahab, E.E.-D.M.A.; Zobia, A.F. Comprehensive Analysis of the Impact of the TCSC on Distance Relays in Interconnected Transmission Networks. *IEEE Access* **2020**, *8*, 228315–228325. [[CrossRef](#)]
29. Das, S.; Santoso, S.; Gaikwad, A.; Patel, M. Impedance-based fault location in transmission networks: Theory and application. *IEEE Access* **2014**, *2*, 537–557. [[CrossRef](#)]
30. Abo-Hamad, G.; Ibrahim, D.; Zahab, E.A.; Zobia, A. Adaptive Mho Distance Protection for Interconnected Transmission Lines Compensated with Thyristor Controlled Series Capacitor. *Energies* **2021**, *14*, 2477. [[CrossRef](#)]
31. Sahoo, B.; Samantaray, S.R. System Integrity Protection Scheme for Enhancing Backup Protection of Transmission Lines. *IEEE Syst. J.* **2021**, *15*, 4578–4588. [[CrossRef](#)]
32. Eissa, M. Developing wide area phase plane primary protection scheme “WA4PS” for complex smart grid system. *Int. J. Electr. Power Energy Syst.* **2018**, *99*, 203–213. [[CrossRef](#)]
33. Hovila, P.; Syväluoma, P.; Kokkonen-Tarkkanen, H.; Horsmanheimo, S.; Borenus, S.; Li, Z.; Uusitalo, M. 5G networks enabling new smart grid protection solutions. In Proceedings of the 25th International Conference on Electricity Distribution: CIRED 2019, Madrid, Spain, 3–6 June 2019; p. 341.